PROCEEDINGS OF THE ROYAL SOCIETY A

FirstCite® e-publishing

Proc. R. Soc. A
doi:10.1098/rspa.2011.0667
Published online

Three-dimensional cellular structures with negative Poisson's ratio and negative compressibility properties

By Joseph N. Grima[1,2,*], Roberto Caruana-Gauci[1], Daphne Attard[1] and Ruben Gatt[1]

[1]*Metamaterials Unit, and* [2]*Department of Chemistry, Faculty of Science, University of Malta, Msida MSD 2080, Malta*

A three-dimensional cellular system that may be made to exhibit some very unusual but highly useful mechanical properties, including negative Poisson's ratio (auxetic), zero Poisson's ratio, negative linear and negative area compressibility, is proposed and discussed. It is shown that such behaviour is scale-independent and may be obtained from particular conformations of this highly versatile system. This model may be used to explain the auxetic behaviour in auxetic foams and in other related cellular systems; such materials are widely known for their superior performance in various practical applications. It may also be used as a blueprint for the design and manufacture of new man-made multifunctional systems, including auxetic and negative compressibility systems, which can be made to have tailor-made mechanical properties.

Keywords: auxetic; negative Poisson's ratio; negative compressibility; analytical model; cellular structure; foams

1. Introduction

The manner in which materials change shape and size when they are subjected to uniaxial stress or pressure is described and quantified by their elastic constants. These elastic constants include the Poisson's ratio, ν_{ij}, a property that describes how the cross section of a material in the $Ox_i - Ox_j$ plane changes its aspect ratio when a uniaxial stress is applied in the Ox_i direction. Mathematically, this property is defined by (Lemprière 1968)

$$\nu_{ij} = -\frac{\varepsilon_j}{\varepsilon_i} \quad (i, j = 1, 2, 3), \tag{1.1}$$

where ε_i is the strain in the Ox_i direction and ε_j is the strain in the orthogonal Ox_j direction. Because most materials get thinner (negative ε_j) when stretched (positive ε_i), the Poisson's ratio is typically a positive property with values such

*Author for correspondence (joseph.grima@um.edu.mt).

Electronic supplementary material is available at http://dx.doi.org/10.1098/rspa.2011.0667 or via http://rspa.royalsocietypublishing.org.

Received 8 November 2011
Accepted 2 May 2012

as +0.3 for steel and +0.5 for rubber. However, it is well known that the Poisson's ratio need not be a positive quantity, and materials having a negative Poisson's ratio, commonly known as auxetics (Evans *et al.* 1991), do exist. In fact, in recent years, there have been several important developments in this field, which led to the prediction, discovery and/or development of several types of auxetic materials (Lakes 1987; Wojciechowski 1989; Evans *et al.* 1991; Grima *et al.* 2000; Alderson *et al.* 2002; Scarpa *et al.* 2005) and structures/models (Gibson *et al.* 1982; Rothenburg *et al.* 1991; Evans *et al.* 1994; Wojciechowski & Branka 1994; Scarpa *et al.* 2004; Grima *et al.* 2005; Alderson & Evans 2009). These include nano-scale materials such as zeolites (Grima *et al.* 2000; Sanchez-Valle *et al.* 2005), silicates (Yeganeh-Haeri *et al.* 1992; Alderson & Evans 2009), cubic materials (Baughman *et al.* 1998*a*; Norris 2006) and liquid crystalline polymers (He *et al.* 1998, 2005); micro-scale materials such as foams (Lakes 1987; Chan & Evans 1997; Alderson *et al.* 2006; Grima *et al.* 2009; Alderson & Alderson 2010; Bianchi *et al.* 2011) and micro-porous polymers (Caddock & Evans 1989; Alderson & Evans 1992; Alderson *et al.* 2002; Ravirala *et al.* 2005); biological systems such as cancellous bone (Williams & Lewis 1982) and macro-scale models based on re-entrant geometries (Gibson *et al.* 1982; Evans *et al.* 1994, 1995; Choi & Lakes 1995; Masters & Evans 1996), chiral structures (Prall & Lakes 1997; Grima *et al.* 2008; Scarpa 2010), rotations of rigid units (Sigmund 1995; Grima & Evans 2000; Grima *et al.* 2005; Alderson & Evans 2009), sliding structures (Rothenburg *et al.* 1991; Wojciechowski & Branka 1994) and hard disks (Wojciechowski 1989; Kowalik & Wojciechowski 2005; Tretiakov & Wojciechowski 2007).

Materials having a negative Poisson's ratio are of interest not only because of a negative Poisson's ratio is in itself a very interesting property, but also because it imparts on the material several other enhanced characteristics that make auxetics superior to their conventional counterparts in many practical applications (Alderson 1999). These enhanced properties range from higher indentation resistance (Lakes & Elms 1993; Alderson *et al.* 1994; Alderson 1999; Webber *et al.* 2008) to synclastic curvature when a bending force is applied (Lakes 1987; Evans 1991; Scarpa *et al.* 2005), and to enhanced sound absorption (Scarpa *et al.* 2003, 2004).

Another important mechanical property that normally assumes positive values is compressibility, a property that defines the way how systems deform when subjected to externally applied hydrostatic pressure p. The isothermal (constant temperature T) volumetric compressibility, β_{V}, which is the inverse of the bulk modulus, and its area or linear equivalents β_{A} and β_{L} may be defined as (Baughman *et al.* 1998*b*)

$$\beta_{\mathrm{V}} = -\frac{1}{V}\left(\frac{\partial V}{\partial p}\right)_T, \quad \beta_{\mathrm{A}} = -\frac{1}{A}\left(\frac{\partial A}{\partial p}\right)_T \quad \text{and} \quad \beta_{\mathrm{L}} = -\frac{1}{L}\left(\frac{\partial L}{\partial p}\right)_T, \tag{1.2}$$

where p is the applied hydrostatic pressure, V is the volume, A is the cross-sectional area in the plane in which the area compressibility is measured and L is the linear dimension along which the linear compressibility is measured.

Compressibility is generally found to be a positive quantity because the dimensions of a material typically decrease with an increase in the externally applied hydrostatic pressure. Until recently, systems with negative volume, area and linear compressibility were given little attention (Baughman *et al.* 1998*b*;

Fortes *et al.* 2011). In fact, systems having the property of negative linear compressibility are seldom reported in the literature, and among others, only few crystal phases (Baughman *et al.* 1998*b*) and tetragonal beam structures (Barnes *et al.* 2012) have been reported to exhibit negative linear compressibility. Lakes also reported open-cell foams with negative bulk modulus (Moore *et al.* 2006) and, together with Wojciechowski, questioned that the bulk modulus has to be positive in all systems, as they proposed that there is no convincing thermodynamic case that negative compressibility of a constrained solid object is inadmissible (Lakes & Wojciechowski 2008). Work by Gatt and Grima also showed that negative apparent linear or area compressibility may be obtained from systems built using more than one component where one of the components responds more to pressure when compared with the others (Gatt & Grima 2008). Negative compressibility materials are predicted to have a number of applications ranging from extremely sensitive pressure detectors, telecommunication line systems, to optical materials with a very high refractive index (Baughman *et al.* 1998*b*).

It was recently highlighted that a two-dimensional system having a honeycomb or wine rack structure may exhibit negative linear compressibility as a consequence of having very high positive Poisson's ratios in certain directions (Grima *et al.* 2011). Although this work is of significant importance in view of the particular applications where negative compressibility materials can be used (Baughman *et al.* 1998*b*), it is limited by the fact that being a two-dimensional system, it is not possible to achieve negative area compressibility, something that may obviously be more useful than negative linear compressibility. Such negative area compressibility resulting from the Poisson's effect is more likely to be achieved when a three-dimensional system exhibits a high positive Poisson's ratio. A system that may be considered as one of the three-dimensional equivalents of the two-dimensional hexagonal honeycomb system is the elongated hexagonal dodecahedron (a 12-sided polyhedron) (Evans *et al.* 1994). This system pertains to a group of model structures that are of great practical importance in view of their ability to represent and model the properties of open-cell foams, including auxetic foams. Such structures include the cubic array of struts of square cross section (Gibson & Ashby 1997) and the regular tetrakaidecahedron (a 14-sided polyhedron) (Choi & Lakes 1995) known to be capable of exhibiting a negative Poisson's ratio in its re-entrant form and a positive Poisson's ratio in its non-re-entrant form, as is the case for the elongated hexagonal dodecahedron (Evans *et al.* 1994). However, the re-entrant form of the tetrakaidecahedron, as proposed by Choi and Lakes is obtained from its non-re-entrant counterpart by a change in geometry of the ribs by substituting some of the straight ribs by kinked ribs so as to provide the re-entrant features that are essential for auxeticity. In contrast to this, the elongated hexagonal dodecahedron structure is obtained from its non-re-entrant counterpart by a change in geometry at the joints so as to convert the Y-shaped joints to arrow-shaped joints.

Despite its relative simplicity, the elongated hexagonal dodecahedron system has not yet been rigorously analysed by analytical or systematic empirical modelling. Here, we present a three-dimensional analytical model that may be used to perform a detailed analysis of a generalized form of the elongated hexagonal dodecahedron structure in an attempt to assess its potential for exhibiting anomalous Poisson's ratios and compressibility properties. In particular, expressions for its mechanical properties, namely Young's moduli

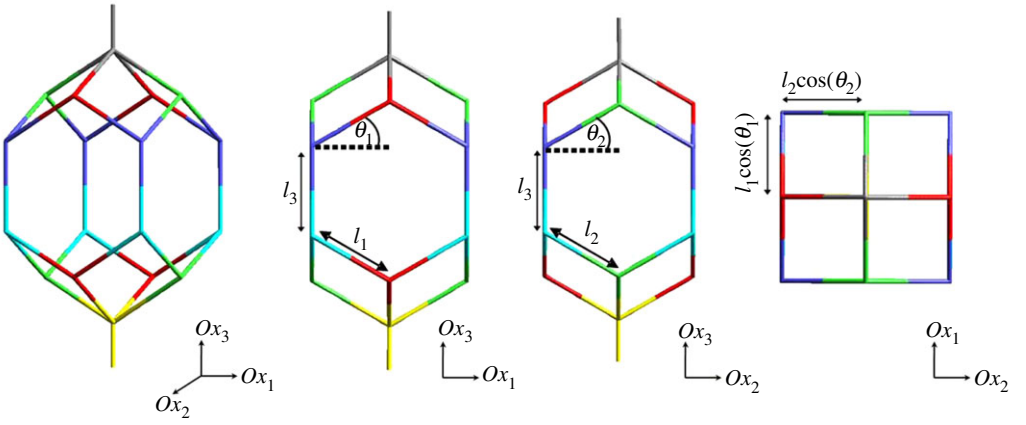

Figure 1. The hexagonal dodecahedron and its two-dimensional projections in the simplest non-re-entrant form for the three major axes. (Online version in colour.)

and Poisson's ratios, for loading on-axis and compressibilities for hydrostatic compressions are derived for this cellular structure deforming through changes in the angles between the cell walls (idealized hinging model), and it is shown that the structure exhibits negative, zero and very large positive Poisson's ratios as well as negative linear and area compressibility for particular conformations.

2. Analytical Model

(*a*) *Structural geometry of the elongated hexagonal dodecahedron*

The structure taken into consideration in this study is a generalized form of the elongated hexagonal dodecahedron. This system is a space-filling structure and may be considered as one of the simplest three-dimensional equivalents of the classical two-dimensional hexagonal honeycomb, with the honeycomb geometry present in two orthogonal planes. Generality in this structure can be achieved by using different angles of the cell and by using different lengths of the cell ribs in different parts of the structure. In particular, the structure modelled is one having dimensions l_3, l_1, l_2, θ_1, θ_2 defined as in figure 1.

The orientation of the structure is such that the unit cell vectors are aligned along the Ox_1, Ox_2 and Ox_3 directions such that the projections of the unit cell in these directions are respectively given by

$$X_1 = 2l_1\cos(\theta_1), \tag{2.1}$$

$$X_2 = 2l_2\cos(\theta_2) \tag{2.2}$$

and

$$X_3 = 2[l_3 + l_1\sin(\theta_1) + l_2\sin(\theta_2)], \tag{2.3}$$

where the geometric parameters are as defined in figure 1. Note that for a structure to be physically realizable, i.e. systems that do not allow the overlap of the ribs, apart from the normal conditions that $l_1 > 0$, $l_2 > 0$, $l_3 \geq 0$, $-90 > \theta_1 > +90$ and $-90 > \theta_2 > +90$, the following three conditions must be satisfied

simultaneously:

$$l_3 + 2l_1 \sin(\theta_1) > 0, \tag{2.4}$$

$$l_3 + 2l_2 \sin(\theta_2) > 0 \tag{2.5}$$

and

$$l_3 + 2l_1 \sin(\theta_1) + 2l_2 \sin(\theta_2) > 0. \tag{2.6}$$

Unless stated otherwise, all the ribs will be assumed to have a circular cross section of diameter $2r$, where r is negligibly small when compared with the other dimensions. Note also that, in general, the cell parameters X_1 and X_2 defined earlier are functions of the variables l_1, l_2, θ_1 and θ_2, i.e.

$$X_i = X_i[l_i, \theta_i], \quad (i = 1, 2), \tag{2.7}$$

and in such systems, the on-axis strains in the Ox_i direction for loading by an infinitesimally small stress $d\sigma_j$ in the Ox_j direction may be defined as

$$d\varepsilon_i^{[j]} = \frac{1}{X_i}\left[\frac{\partial X_i}{\partial l_1} dl_1^{[j]} + \frac{\partial X_i}{\partial l_2} dl_2^{[j]} + \frac{\partial X_i}{\partial \theta_1} d\theta_1^{[j]} + \frac{\partial X_i}{\partial \theta_2} d\theta_2^{[j]}\right], \quad (j = 1, 2, 3), \tag{2.8}$$

where $dl_1^{[j]}$, $dl_2^{[j]}$, $d\theta_1^{[j]}$ and $d\theta_2^{[j]}$ represent how much the parameters l_1, l_2, θ_1 and θ_2 change when subjected to the stress $d\sigma_j$ and can be expressed in terms of the applied stress $d\sigma_j$ through the hinging stiffness constant as discussed later. Note that the superscript $[j]$ is used to denote that the stress is being applied in the Ox_j direction.

(*b*) *The on-axis mechanical properties*

This section presents a derivation of the on-axis Poisson's ratios and Young's moduli of idealized systems that deform solely through changes in the angles between the ribs—that is, the idealized hinging model.

In this derivation, for the idealized hinging model, it shall be assumed that the hinges in the structure that are associated with the angles θ_1 and θ_2 (i.e. hinges at each end of the inclined ribs which connect the ribs with a hypothetical horizontal line) are simple two-dimensional hinges that have an associated stiffness constant k_h defined by

$$M = k_\mathrm{h} \delta\theta, \tag{2.9}$$

where M is the moment that generates the change in the angles from θ to $\theta + \delta\theta$.

In addition, the geometric parameters l_1 and l_2 will be assumed to remain constant through the deformations, i.e. there is no stretching of the ribs and thus the strain equation (2.8) simplifies to

$$d\varepsilon_i^{[j]} = \frac{1}{X_i}\left[\frac{\partial X_i}{\partial \theta_1} d\theta_1^{[j]} + \frac{\partial X_i}{\partial \theta_2} d\theta_2^{[j]}\right], \tag{2.10}$$

where the terms $d\theta_1^{[j]}$ and $d\theta_2^{[j]}$ may be expressed in terms of the applied stress $d\sigma_j$ by considering the magnitude of the moments that result in these changes in angles. The on-axis strains in the Ox_i direction for loading by an infinitesimally small stress $d\sigma_j$ in the Ox_j direction thus simplify to

— Loading in the Ox_1 direction:

$$d\varepsilon_1^{[1]} = \frac{1}{4k_h}\frac{X_2X_3}{X_1}l_1^2\sin^2(\theta_1)\,d\sigma^{[1]}, \tag{2.11}$$

$$d\varepsilon_2^{[1]} = 0 \tag{2.12}$$

and

$$d\varepsilon_3^{[1]} = -\frac{1}{4k_h}X_2l_1^2\sin(\theta_1)\cos(\theta_1)\,d\sigma^{[1]}. \tag{2.13}$$

— Loading in the Ox_2 direction:

$$d\varepsilon_1^{[2]} = 0, \tag{2.14}$$

$$d\varepsilon_2^{[2]} = \frac{1}{4k_h}\frac{X_1X_3}{X_2}l_2^2\sin^2(\theta_2)\,d\sigma^{[2]} \tag{2.15}$$

and

$$d\varepsilon_3^{[2]} = -\frac{1}{4k_h}X_1l_2^2\sin(\theta_2)\cos(\theta_2)\,d\sigma^{[2]}. \tag{2.16}$$

— Loading in the Ox_3 direction:

$$d\varepsilon_1^{[3]} = -\frac{1}{4k_h}X_2l_1^2\sin(\theta_1)\cos(\theta_1)\,d\sigma^{[3]}, \tag{2.17}$$

$$d\varepsilon_2^{[3]} = -\frac{1}{4k_h}X_1l_2^2\sin(\theta_2)\cos(\theta_2)\,d\sigma^{[3]} \tag{2.18}$$

and

$$d\varepsilon_3^{[3]} = \frac{1}{4k_h}\frac{X_1X_2}{X_3}[l_1^2\cos^2(\theta_1) + l_2^2\cos^2(\theta_2)]d\sigma^{[3]}. \tag{2.19}$$

Hence, Young's moduli E_j for loading in the Ox_j direction and Poisson's ratios ν_{ji} in the $Ox_i - Ox_j$ plane for loading in the Ox_j direction are given by

— Loading in the Ox_1 direction:

$$E_1 = \frac{d\sigma^{[1]}}{d\varepsilon_1^{[1]}} = 4k_h\frac{X_1}{X_2X_3}\frac{1}{l_1^2\sin^2(\theta_1)}, \tag{2.20}$$

$$\nu_{12} = -\frac{d\varepsilon_2^{[1]}}{d\varepsilon_1^{[1]}} = 0 \tag{2.21}$$

and

$$\nu_{13} = -\frac{d\varepsilon_3^{[1]}}{d\varepsilon_1^{[1]}} = \frac{X_1}{X_3}\cot(\theta_1) \tag{2.22}$$

— Loading in the Ox_2 direction:

$$E_2 = \frac{d\sigma^{[2]}}{d\varepsilon_2^{[2]}} = 4k_h\frac{X_2}{X_1X_3}\frac{1}{l_2^2\sin^2(\theta_2)}, \tag{2.23}$$

$$\nu_{21} = -\frac{d\varepsilon_1^{[2]}}{d\varepsilon_2^{[2]}} = 0 \tag{2.24}$$

and

$$\nu_{23} = -\frac{d\varepsilon_3^{[2]}}{d\varepsilon_2^{[2]}} = \frac{X_2}{X_3}\cot(\theta_2). \tag{2.25}$$

— Loading in the Ox_3 direction:

$$E_3 = \frac{d\sigma^{[3]}}{d\varepsilon_3^{[3]}} = 4k_{\mathrm{h}} \frac{X_3}{X_1 X_2} \frac{1}{\left[l_1^2 \cos^2(\theta_1) + l_2^2 \cos^2(\theta_2)\right]}, \tag{2.26}$$

$$\nu_{31} = -\frac{d\varepsilon_1^{[3]}}{d\varepsilon_3^{[3]}} = \frac{X_3}{X_1} \frac{l_1^2 \sin(\theta_1)\cos(\theta_1)}{l_1^2 \cos^2(\theta_1) + l_2^2 \cos^2(\theta_2)} \tag{2.27}$$

and

$$\nu_{32} = -\frac{d\varepsilon_2^{[3]}}{d\varepsilon_3^{[3]}} = \frac{X_3}{X_2} \frac{l_2^2 \sin(\theta_2)\cos(\theta_2)}{l_1^2 \cos^2(\theta_1) + l_2^2 \cos^2(\theta_2)}. \tag{2.28}$$

(*c*) *Compressibility*

Having determined Young's moduli and Poisson's ratios, one may obtain expressions for $\beta_{\mathrm{L}}[Ox_i]$, the linear compressibility in the Ox_i direction, which is defined by

$$\beta_{\mathrm{L}}[Ox_i] = -\left(\frac{d\varepsilon_i^{[1]} + d\varepsilon_i^{[2]} + d\varepsilon_i^{[3]}}{dp}\right)_T, \tag{2.29}$$

where dp is an infinitesimal hydrostatic pressure change, which corresponds to a situation where $dp = d\sigma^{[1]} = d\sigma^{[2]} = d\sigma^{[3]}$. This expression may be expressed in terms of the Poisson's ratios and Young's moduli to obtain

$$\beta_{\mathrm{L}}[Ox_1] = \frac{1}{E_1} - \left(\frac{\nu_{21}}{E_2} + \frac{\nu_{31}}{E_3}\right), \tag{2.30}$$

$$\beta_{\mathrm{L}}[Ox_2] = \frac{1}{E_2} - \left(\frac{\nu_{12}}{E_1} + \frac{\nu_{32}}{E_3}\right) \tag{2.31}$$

and

$$\beta_{\mathrm{L}}[Ox_3] = \frac{1}{E_3} - \left(\frac{\nu_{13}}{E_1} + \frac{\nu_{23}}{E_2}\right). \tag{2.32}$$

These expressions may then be used to obtain the equivalent expression for $\beta_{\mathrm{A}}[Ox_i - Ox_j]$, the area compressibility in the $Ox_i - Ox_j$ plane, which is defined by

$$\beta_{\mathrm{A}}[Ox_i - Ox_j] = \beta_{\mathrm{L}}[Ox_i] + \beta_{\mathrm{L}}[Ox_j], \tag{2.33}$$

and β_{V}, the volumetric compressibility, which is defined by

$$\beta_{\mathrm{V}} = \beta_{\mathrm{L}}[Ox_1] + \beta_{\mathrm{L}}[Ox_2] + \beta_{\mathrm{L}}[Ox_3], \tag{2.34}$$

Note that these expressions may be rewritten in terms of the Poisson's ratios and Young's moduli by substituting equations (2.30)–(2.32) in equations (2.33) and (2.34), thus for example

$$\beta_{\mathrm{A}}[Ox_1 - Ox_2] = \left(\frac{1}{E_1} + \frac{1}{E_2}\right) - \left(\frac{\nu_{21}}{E_2} + \frac{\nu_{31}}{E_3} + \frac{\nu_{12}}{E_1} + \frac{\nu_{32}}{E_3}\right) \tag{2.35}$$

and

$$\beta_{\mathrm{V}} = \left(\frac{1}{E_1} + \frac{1}{E_2} + \frac{1}{E_3}\right) - 2\left(\frac{\nu_{12}}{E_1} + \frac{\nu_{23}}{E_2} + \frac{\nu_{31}}{E_3}\right). \tag{2.36}$$

Note that these expressions suggest that this system has the potential to exhibit negative compressibilities if the terms with the negative sign are larger than the positive terms involving solely the reciprocal of the moduli. This condition would obviously be more likely to be met by systems having very large positive Poisson's ratios.

For the presented structure, the expressions for linear compressibility when the system deforms through the idealized hinging model may be obtained by substituting equations (2.20)–(2.28) in equations (2.30)–(2.32) to obtain

$$\beta_{\mathrm{L}}[Ox_1] = \frac{X_2 l_1^2}{4k_{\mathrm{h}}}\left(\frac{X_3}{X_1}\sin^2(\theta_1) - \cos(\theta_1)\sin(\theta_1)\right), \tag{2.37}$$

$$\beta_{\mathrm{L}}[Ox_2] = \frac{X_1 l_2^2}{4k_{\mathrm{h}}}\left(\frac{X_3}{X_2}\sin^2(\theta_2)\sin(\theta_2)\cos(\theta_2)\right) \tag{2.38}$$

and

$$\beta_{\mathrm{L}}[Ox_3] = \frac{1}{4k_{\mathrm{h}}}\left\{\frac{X_1 X_2}{X_3}[l_1^2\cos^2(\theta_1) + l_2^2\cos^2(\theta_2)] - [X_2 l_1^2\sin(\theta_1)\cos(\theta_1) + X_1 l_2^2\sin(\theta_2)\cos(\theta_2)]\right\} \tag{2.39}$$

Note that in the case when $l_1 = l_2 = l$ and $\theta_1 = \theta_2 = \theta$ (i.e. $X_1 = X_2$), the expressions for the linear compressibility simplify to

$$\beta_{\mathrm{L}}[Ox_1] = \beta_{\mathrm{L}}[Ox_2] = \frac{l^2}{4k_{\mathrm{h}}}(X_3\sin^2(\theta) - X_1\cos(\theta)\sin(\theta)) \tag{2.40}$$

and

$$\beta_{\mathrm{L}}[Ox_3] = \frac{l^2}{2k_{\mathrm{h}}}\left[\frac{X_1^2}{X_3}\cos^2(\theta) - X_1\sin(\theta)\cos(\theta)\right]. \tag{2.41}$$

The equations (2.37)–(2.39) may then be added accordingly to obtain the expressions for β_{A} and β_{V}.

3. Results and discussion

Typical contour plots of Young's moduli, Poisson's ratios and compressibility (linear, area and volumetric) obtained from the analytical model are shown in figures 2 and 3, wherein non-greyed-out regions correspond to physically realizable structures.

An analysis of the equations and plots for the idealized hinging system suggests that the system exhibits negative Poisson's ratios in the $Ox_1 - Ox_3$ and $Ox_2 - Ox_3$ planes whenever the angle in that particular plane is negative, and positive Poisson's ratios in the same planes whenever the angle in that particular plane is positive. That is, if both the angles θ_1 and θ_2 in the $Ox_1 - Ox_3$ and $Ox_2 - Ox_3$ planes are negative, i.e. the geometry is re-entrant in both these planes, then the system will exhibit negative on-axis Poisson's ratio in these two planes. Similarly,

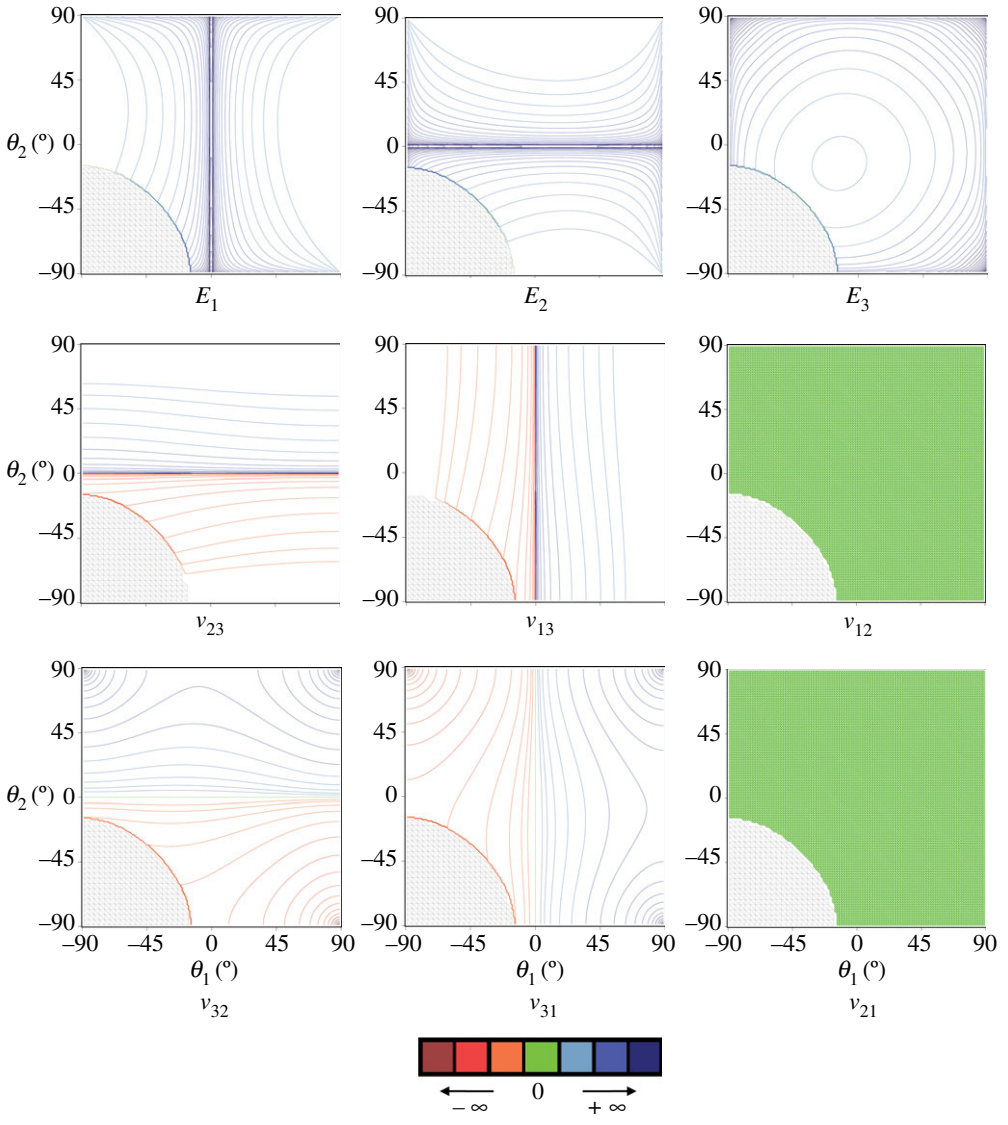

Figure 2. Contour plots obtained from the analytical model for Young's moduli and the Poisson's ratios for a system with $l_3 = 0.5$ nm, $l_1 = 0.2$ nm and $l_2 = 0.2$ nm. (Online version in colour.)

if both the angles θ_1 and θ_2 in the $Ox_1 - Ox_3$ and $Ox_2 - Ox_3$ planes are positive, i.e. the geometry is non-re-entrant in both these planes, then the system will exhibit positive Poisson's ratio in these two planes. All this is as expected, and may be inferred from an extrapolation of the existent two-dimensional hinging model if transposed to three-dimensional (Evans *et al.* 1994).

Also of interest is the fact that independently of the sign or magnitude of the angles θ_1 and θ_2, and of the magnitude of the other geometric parameters l_1, l_2 and l_3, the Poisson's ratios ν_{12} and ν_{21} in the $Ox_1 - Ox_2$ plane are always zero. This behaviour may be regarded as anomalous in view of the fact that it may occur

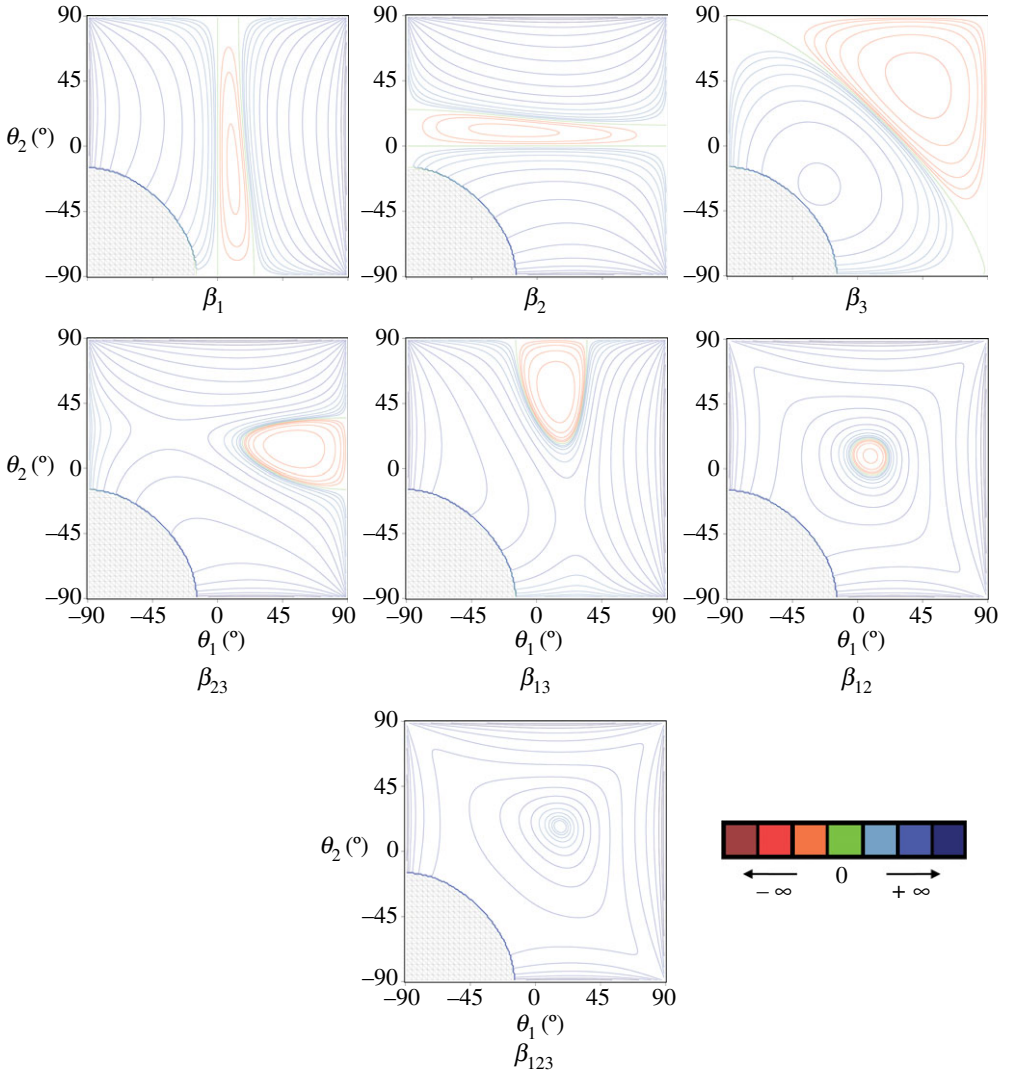

Figure 3. Contour plots obtained from the analytical model for the linear, area and volume compressibility for a system with $l_3 = 0.5$ nm, $l_1 = 0.2$ nm and $l_2 = 0.2$ nm. (Online version in colour.)

for a wide range of applied strain, i.e. it is not solely observed in a small-strain region as the system goes from a negative Poisson's ratio to a positive Poisson's ratio, as is normally the case. Instead, the system studied here always exhibits zero Poisson's ratio in the $Ox_1 - Ox_2$ plane through all the angles of deformation. Such a feature could not be extrapolated from the existent two-dimensional model and is of particular practical importance in view of the fact that systems with zero or near-zero Poisson's ratio are of great practical importance in their own accord (Attard & Grima 2010) and are a characteristic of some foams under high compressive strains. Here, it should be noted that zero Poisson's ratios occur in foams and in centre-symmetric honeycombs when the cells are straightened

along the loading direction, something that prima facie may be regarded as a stretching deformation mechanism. In this respect, it is interesting to note that that if one had to look at the two-dimensional projection of the $Ox_1 - Ox_2$ plane, then the hinging deformation observed here would have become equivalent to 'a stretching-like' mechanism.

As a corollary of all this, any system that has a negative angle in only one of the $Ox_1 - Ox_3$ and $Ox_2 - Ox_3$ planes will exhibit negative, zero and positive on-axis Poisson's ratios in its major $Ox_1 - Ox_2$, $Ox_1 - Ox_3$ and $Ox_2 - Ox_3$ planes, something that to the authors' knowledge has not been highlighted before and will occur for a wide range of θ values and hence strains. In particular, in such systems, the auxeticity occurs in the plane where the angle is negative, the ever present zero Poisson's ratio occurs in the $Ox_1 - Ox_2$ plane and the positive Poisson's ratio occurring in the plane where the angle is positive. Such a structure is possible owing to the particular three-dimensional geometry of the system where the values of θ_1 and θ_2 are fully independent of each other. It should also be noted that as clearly illustrated by equations (2.20)–(2.28) and by figures 2 and 3, the mechanical properties of this system can be fine-tuned through careful choice of the geometric parameters l_i as well θ_i, which have a significant effect on the mechanical properties of this system, as discussed in detail in the electronic supplementary material.

At this point, it would be interesting to compare the expressions for the Poisson's ratios derived here with those derived for the simpler two-dimensional version of the hinging honeycombs (Evans *et al.* 1994). Referring to figure 4, one may note that the vertical y-direction in the two-dimensional model corresponds to the Ox_3 direction in our model, while the horizontal x-direction in the two-dimensional model corresponds to the Ox_i $(i = 1, 2)$ directions in our model. Thus, it would be appropriate to compare our expressions for ν_{i3} and ν_{3i} with the two-dimensional ν_{xy} and ν_{yx} respectively, whose Poisson's ratios are given by (Evans *et al.* 1994):

$$\nu_{xy} = \frac{\cos^2(\theta)}{\sin(\theta)}\left[\frac{1}{h/l + \sin(\theta)}\right] \tag{3.1}$$

and

$$\nu_{yx} = \frac{\sin(\theta)}{\cos^2(\theta)}\left[\frac{h}{l} + \sin(\theta)\right]. \tag{3.2}$$

The first noticeable thing is that whereas in the two-dimensional version, $\nu_{xy} = 1/\nu_{yx}$, this is not the case in the three-dimensional model, where $\nu_{i3} \neq 1/\nu_{3i}$ something that clearly explains the limitations already highlighted when transposing the published two-dimensional model to the three-dimensional structure (Evans *et al.* 1994). In fact, although the expressions for ν_{i3} are roughly equivalent to those of ν_{xy}, something that may be explained by considering that loading on Ox_i $(i = 1, 2)$ will only result in change in the angle θ_i and not the other, this is not the case for ν_{3i} and ν_{yx}, where the expression for ν_{3i} is much more complex than ν_{yx} and where loading in Ox_3 will result in changes in both θ_1 and θ_2.

Having analysed the Poisson's ratios, we can now consider compressibility properties. As clearly highlighted in equations (2.30)–(2.34) and the plots in figure 3, for certain conditions, the idealized hinging system can exhibit both

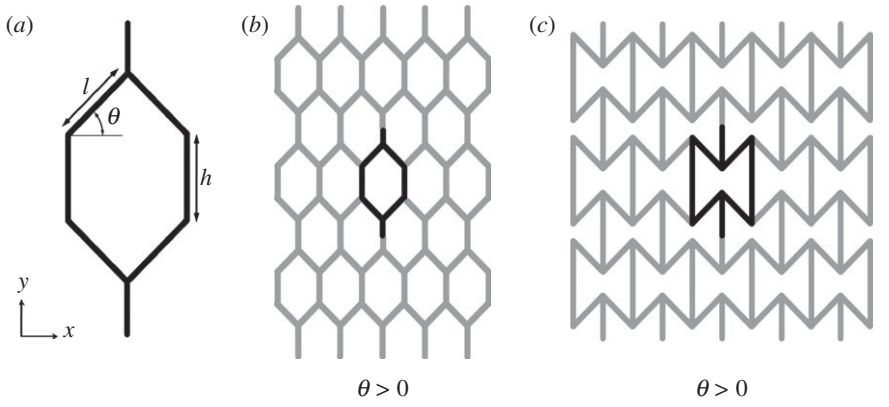

Figure 4. (*a*) Variables defining the geometry of a two-dimensional honeycomb: when (*b*) $\theta > 0$ the honeycomb is considered to be a conventional honeycomb, whereas when (*c*) $\theta < 0$ this is termed re-entrant honeycomb.

negative linear compressibility and negative area compressibility. The equation for the on-axis linear compressibility is given by

$$\beta_{\mathrm{L}}[Ox_j] = \frac{1}{E_j} - \left(\sum_{i=1}^{3} \frac{\nu_{ij}}{E_i} (1 - \delta_{ij}) \right), \tag{3.3}$$

where δ_{ij} is the Kronecker delta. This equation shows that negative linear compressibility is achievable whenever $\nu_{ij} > E_i/E_j$, something that is realizable only for systems having large positive Poisson's ratios as in the case of some of the studied systems with the non-re-entrant features undergoing a hinging type deformation mechanism.

If we first analyse the simplified system where $l_1 = l_2 = l$ and $\theta_1 = \theta_2 = \theta$, we note that because the system will only be non-auxetic in the region where $0° < \theta < 90°$, then the expressions for linear compressibility using equations (2.30)–(2.32) will have to satisfy the following conditions in order to exhibit negative compressibility:

$$\text{(a) for negative } \beta_{\mathrm{L}}[Ox_1] = \beta_{\mathrm{L}}[Ox_2] \quad \frac{l\cos(\theta)}{l_3 + 2l\sin(\theta)} > \tan(\theta) \tag{3.4}$$

and

$$\text{(b) for negative } \beta_{\mathrm{L}}[Ox_3] \quad \frac{l\cos(\theta)}{l_3 + 2l\sin(\theta)} < \tan(\theta), \tag{3.5}$$

which clearly suggests that in this highly symmetric system, negative compressibility in the Ox_1 and Ox_2 directions (which occur concurrently due to the symmetry) will arise at the exclusion of negative compressibility in the Ox_3 direction, and vice versa. Also of interest is the fact that these equations suggest zero compressibility in the three orthogonal directions, i.e.

$$\beta_{\mathrm{L}}[Ox_1] = \beta_{\mathrm{L}}[Ox_2] = \beta_{\mathrm{L}}[Ox_3] = 0, \quad \text{if} \quad \frac{l\cos(\theta)}{l_3 + 2l\sin(\theta)} = \tan(\theta), \tag{3.6}$$

whose condition corresponds to the turning point in the plots of the linear compressibilities against θ. Similar behaviour could be observed for the two-dimensional hexagonal systems (Grima *et al.* 2011) although obviously the turning points occur at different geometric conditions.

For the idealized hinging system when $l_1 = l_2 = l$ and $\theta_1 = \theta_2 = \theta$, hence $\beta_L[Ox_1] = \beta_L[Ox_2]$, the conditions for negative area compressibility in the $Ox_1 - Ox_2$ plane are given by equation (3.4). In the case of the $Ox_1 - Ox_3$ and $Ox_2 - Ox_3$ planes, because the two mutually orthogonal linear compressibilities in the respective planes have different signs, then the situation is more complex although it may be shown that the area compressibilities in these planes are negative in the narrow range between θ values obtained by solving the equation

$$\beta_L[Ox_i] + \beta_L[Ox_3] = 0; \tag{3.7}$$

this has the roots given by

$$\frac{l\cos(\theta)}{l_3 + 2l\sin(\theta)} = \tan(\theta) \quad \text{and} \quad \frac{2l\cos(\theta)}{l_3 + 2l\sin(\theta)} = \tan(\theta). \tag{3.8}$$

It may also be shown that the proposed systems may never exhibit negative volumetric compressibility values because if one had to solve the equation

$$\beta_V = \beta_L[Ox_1] + \beta_L[Ox_2] + \beta_L[Ox_3] = 0, \tag{3.9}$$

one would find that this expression has a double root when

$$\frac{l\cos(\theta)}{l_3 + 2l\sin(\theta)} = \tan(\theta), \tag{3.10}$$

that is, the volumetric compressibility is always positive except at the point when the earlier-mentioned equation is satisfied. In this case, the volumetric compressibility is zero because the roots coincide (i.e. the range of possible negative values of β_V is non-existent).

Although all this is of great interest, particularly in view of the fact that negative linear or area compressibilities are not commonly encountered, it should be noted that even more interesting properties may be obtained from the general case. Although it is not the scope of this work to fully scrutinize this system, it is important to highlight that as easily inferred from the plots in figures 2 and 3, in general it is possible for a system to be both auxetic and have negative linear and even area compressibility. This behaviour is possible because the $Ox_1 - Ox_3$ and $Ox_2 - Ox_3$ planes are fully independent of each other and it is possible to have one plane exhibiting auxetic behaviour and another plane exhibiting conventional behaviour (a requirement for negative compressibility of this type). However, at this point, it is important to emphasize that for negative compressibility to be observed through the mechanism discussed in this paper, the hydrostatic pressure on the system must be applied in such a way that the pressure is felt only by the outer surface of the system and not by the inner surface of the cell walls themselves. In other words, if for example, the pressure is exerted through a fluid, then the system must effectively behave as a non-porous system vis-à-vis this fluid, i.e. the pores of the system must be smaller than the dimensions of the fluid particles so as to ensure that the fluid that is exerting the hydrostatic pressure on the system cannot penetrate into the system and exert pressure from the inside.

Furthermore, one should highlight the fact that the negative compressibility reported in this paper relates only to linear or area compressibility, properties that have also been found to occur in real materials such as methanol monohydrate (Fortes *et al.* 2011). Such properties need not be associated to unstable systems especially because the overall volume compressibility is always positive.

More practically, one should highlight the fact that the work presented here is of interest not only because it defines necessary conditions for obtaining negative Poisson's ratio and/or negative compressibility, two very unusual but highly useful mechanical properties that may occur concurrently, but also in view of the potential role that this model may have in real everyday applications. In particular, it should be noted that recent studies relating to the micro-structural features of auxetic open-cell foams have shown that rib hinging is one of the mechanisms that leads to auxetic behaviour in these foams (McDonald *et al.* 2009) and it is a known fact that most foams exhibit near-zero Poisson's ratios under high compressive strains, a property that is representable by this model. Obviously, in such real systems it may be unrealistic to assume that the real material would behave in the highly idealized manner presented here, i.e. that the foam deforms solely through changes in the angles between the ribs (idealized hinging model). For example, it is more likely that in real systems, hinging is accompanied by other concurrent modes of deformation, such as stretching or flexure of the ribs (Masters & Evans 1996; Gibson & Ashby 1997), and even rotation of joints (Grima *et al.* 2005). Such mechanisms would act alongside the hinging mechanism presented here with the result that the overall mechanical properties observed could deviate from the values predicted by this idealized model. In fact, in such a real system, the overall observed mechanical properties would depend on the relative dominance of the different mechanisms.

In addition, deviations from ideality may even be more poignant when one applies the model presented here to materials with micro- or nanostructures that have some degree of irregularity, as is the case in open-cell foams. In fact, although the elongated hexagonal dodecahedron geometry has been proposed as a possible model of foam materials (Evans *et al.* 1994), in view of the fact that like real foam cells, the elongated hexagonal dodecahedron cell is space-filling and its elongated features may adequately represent the rise direction present in foams, one may argue that this model is still over simplistic as it is highly symmetric and ordered. Thus, it is remarkable that despite its simplicity, the model presented here may be used to explain some commonly observed properties of foams, such as the occurrence of near-zero Poisson's ratios that are observed in some auxetic foams (Lakes 1987; Scarpa *et al.* 2005) and in certain conventional foams under high compressive strains (Choi & Lakes 1992; Bezazi & Scarpa 2007; Dawson *et al.* 2007) or the negative Poisson's ratios in auxetic foams even though the perfection presented in this model is rarely observed in real cellular systems that are normally characterized by irregular poly-dispersed cells.

Before concluding, one should highlight the fact that there is no constraint on the actual value that the geometric parameters l_1, l_2 and l_3 may assume, i.e. the presented geometry-deformation mechanism model is scale-independent. This means that the proposed model may be used as a blueprint in the design, synthesis and/or manufacture of man-made multifunctional materials, which may be constructed at the macro-scale, micro-scale as well as at the nano-scale using, for example, micro-fabrication techniques such as laser ablation, selective

electron-beam melting and stereolithography. In such work, the model proposed here would be able to provide invaluable information as it would be able to give an estimate of the relative internal dimensions that need to be used to attain a material that exhibits some pre-desired set of mechanical properties with the result that materials can be tailor-made for specific practical applications.

4. Conclusion

An analytical model was presented for the elongated hexagonal dodecahedron deforming through the hinging mechanism (i.e. solely through changes in the angles between the ribs) where the conditions for this system to exhibit atypical properties such as negative Poisson's ratio or negative compressibility (linear and/or area) were specified.

It was shown that a negative Poisson's ratio is obtained whenever the geometry in that particular plane is in the re-entrant form. On the other hand, the system exhibits a positive Poisson's ratio in the same planes whenever the geometry is in the non-re-entrant form. It was also shown that the system always exhibits the rare property of a zero on-axis Poisson's ratio through all angles of deformation in one of its planes, something that is of importance because very few structures have been proposed to exhibit zero Poisson's ratio through such a wide range of deformation. Because the angles between the ribs present in different planes are fully independent from each other, the proposed system is so versatile that it may exhibit concurrent positive, zero and/or negative Poisson's ratios in different planes at the same time, something that could not be easily deduced from the earlier-published two-dimensional models of this system.

It was also shown that the structure may also exhibit the unusual property of negative linear compressibility when at least one of its planes has the non-re-entrant geometry satisfying certain conditions, and may even exhibit negative area compressibility when several more stringent conditions are also satisfied. This latter property is even less encountered than negative linear compressibility.

Given the many useful properties associated with systems exhibiting negative Poisson's ratio and/or negative compressibility, and the fact that this proposed model as discussed before may be very useful to explain some properties of open-cell foams or as a blueprint for the design and manufacture of novel man-made multifunctional materials, it is hoped that the work presented here will be useful to scientists and engineers working in the design and manufacture of new man-made auxetics and related materials that exhibit superior macroscopic properties.

The financial support of the Malta Council for Science and Technology through their 2008 R&I scheme is gratefully acknowledged as is the support of Methode Electronics (Malta) Ltd., who are partners in this project. The authors also thank the University of Malta.

References

Alderson, A. 1999 A triumph of lateral thought. *Chem. Ind.* (*Lond.*) **384**, 384–391.

Alderson, A. & Alderson, K. L. 2010 Developments in auxetic foams. In *3rd Int. Conf. 7th International Workshop on Auxetics & Related Systems, Gozo and Malta, 19–23 July 2010*, p. 210. Gdansk, Poland: TASK Publishing.

Alderson, K. L. & Evans, K. E. 1992 The fabrication of microporous polyethylene having a negative Poisson's ratio. *Polymer* **33**, 4435–4438. (doi:10.1016/0032-3861(92)90294-7)

Alderson, A. & Evans, K. E. 2009 Deformation mechanisms leading to auxetic behaviour in the α-cristobalite and α-quartz structures of both silica and germania. *J. Phys. Condens. Matter* **21**, 025401. (doi:10.1088/0953–8984/21/2/025401)

Alderson, K. L., Pickles, A. P., Neale, P. J. & Evans, K. E. 1994 Auxetic polyethylene: the effect of a negative Poisson's ratio on hardness. *Acta Metall. Mater.* **42**, 2261–2266. (doi:10.1016/0956-7151(94)90304-2)

Alderson, K. L., Alderson, A., Smart, G., Simkins, V. R. & Davies, P. J. 2002 Auxetic polypropylene fibres. I. Manufacture and characterisation. *Plast. Rubber Compos.* **31**, 344–349. (doi:10.1179/146580102225006495)

Alderson, A., Alderson, K. L., Davies, P. J. & Smart, G. M. 2006 *Process for the preparation of auxetic foams*. US Patent no. 20100029796.

Attard, D. & Grima, J. N. 2010 Modelling of hexagonal honeycombs exhibiting zero Poisson's ratio. *Phys. Status Solidi B* **248**, 52–59. (doi:10.1002/pssb.201083980)

Barnes, D. L., Miller, W., Evans, K. E. & Marmier, A. S. H. 2012 Modelling negative linear compressibility in tetragonal beam structures. *Mech. Mater.* **46**, 123–128. (doi:10.1016/j.mechmat.2011.12.007)

Baughman, R. H., Shacklette, J. M., Zakhidov, A. A. & Stafstrom, S. 1998*a* Negative Poisson's ratios as a common feature of cubic metals. *Nature* **392**, 362–365. (doi:10.1038/32842)

Baughman, R. H., Stafstrom, S., Cui, C. & Dantas, S. O. 1998*b* Materials with negative compressibilities in one or more dimensions. *Science* **279**, 1522–1524. (doi:10.1126/science.279.5356.1522)

Bezazi, A. & Scarpa, F. 2007 Mechanical behaviour of conventional and negative Poisson's ratio thermoplastic polyurethane foams under compressive cyclic loading. *Int. J. Fatigue* **29**, 922–930. (doi:10.1016/j.ijfatigue.2006.07.015)

Bianchi, M., Scarpa, F., Banse, M. & Smith, C. W. 2011 Novel generation of auxetic open-cell foams for curved and arbitrary shapes. *Acta Mater.* **59**, 686–691. (doi:10.1016/j.actamat.2010.10.006)

Caddock, B. D. & Evans, K. E. 1989 Microporous materials with negative Poisson's ratio I: microstructure and mechanical properties. *J. Phys. D Appl. Phys.* **22**, 1877–1882. (doi:10.1088/0022-3727/22/12/012)

Chan, N. & Evans, K. E. 1997 Fabrication methods for auxetic foams. *J. Mater. Sci.* **32**, 5945–5953. (doi:10.1023/A:1018606926094)

Choi, J. B. & Lakes, R. S. 1992 Nonlinear properties of polymer cellular materials with a negative Poisson's ratio. *J. Mater. Sci.* **27**, 4678–4684. (doi:10.1007/BF01166005)

Choi, J. B. & Lakes, R. S. 1995 Analysis of elastic modulus of conventional foams and of re-entrant foam materials with a negative Poisson's ratio. *Int. J. Mech. Sci.* **37**, 51–59. (doi:10.1016/0020-7403(94)00047-N)

Dawson, M. A., Germaine, J. T. & Gibson, L. J. 2007 Permeability of open-cell foams under compressive strain. *Int. J. Solids Struct.* **44**, 5133–5145. (doi:10.1016/j.ijsolstr.2006.12.025)

Evans, K. E. 1991 The design of doubly curved sandwich panels with honeycomb-cores. *Compos. Struct.* **17**, 95–111. (doi:10.1016/0263-8223(91)90064-6)

Evans, K. E., Nkansah, M. A., Hutchinson, I. J. & Rogers, S. C. 1991 Molecular network design. *Nature* **353**, 124–125. (doi:10.1038/353124a0)

Evans, K. E., Nkansah, M. A. & Hutchinson, I. J. 1994 Auxetic foams: modelling negative Poisson's ratios. *Acta Metall. Mater.* **42**, 1289–1294. (doi:10.1016/0956-7151(94)90145-7)

Evans, K. E., Alderson, A. & Christian, F. R. 1995 Auxetic two-dimensional polymer networks: an example of tailoring geometry for specific mechanical properties. *J. Chem. Soc. Faraday Trans.* **91**, 2671–2680. (doi:10.1039/ft9959102671)

Fortes, A. D., Suard, E. & Knight, K. S. 2011 Negative linear compressibility and massive anisotropic thermal expansion in methanol monohydrate. *Science* **331**, 742–746. (doi:10.1126/science.1198640)

Gatt, R. & Grima, J. N. 2008 Negative compressibility. *Phys. Status Solidi RRL* **2**, 236–238. (doi:10.1002/pssr.200802101)

Gibson, L. J. & Ashby, M. F. 1997 *Cellular solids structure and properties*, 2nd edn. pp. 94–98. Cambridge, UK: Cambridge University Press.

Gibson, L. J., Ashby, M. F., Schajer, G. S. & Robertson, C. I. 1982 The mechanics of two-dimensional cellular materials. *Proc. R. Soc. Lond. A* **382**, 25–42. (doi:10.1098/rspa.1982.0087)

Grima, J. N. & Evans, K. E. 2000 Auxetic behaviour from rotating squares. *J. Mater. Sci. Lett.* **19**, 1563–1565. (doi:10.1023/A:1006781224002)

Grima, J. N., Jackson, R., Alderson, A. & Evans, K. E. 2000 Do zeolites have negative Poisson's ratios? *Adv. Mater.* **12**, 1912–1918. (doi:10.1002/1521-4095(200012)12:24<1912::AID-ADMA1912>3.0.CO;2-7)

Grima, J. N., Alderson, A. & Evans, K. E. 2005 An alternative explanation for the negative Poisson's ratios in auxetic foams. *J. Phys. Soc. Jpn.* **74**, 1341–1342. (doi: 10.1143/JPSJ.74.1341)

Grima, J. N., Gatt, R. & Farrugia, P. S. 2008 On the properties of auxetic meta-tetrachiral structures. *Phys. Status Solidi B Basic Res.* **245**, 511–520. (doi:10.1002/pssb.200777704)

Grima, J. N., Attard, D., Gatt, R. & Cassar, R. N. 2009 A novel process for the manufacture of auxetic foams and for their reconversion to conventional form. *Adv. Eng. Mater.* **11**, 533–535. (doi:10.1002/macp.200400302)

Grima, J. N., Attard, D., Caruana-Gauci, R. & Gatt, R. 2011 Negative linear compressibility of hexagonal honeycombs and related systems. *Scr. Mater.* **65**, 565–568. (doi:10.1016/j.scriptamat.2011.06.011)

He, C., Liu, P. & Griffin, A. C. 1998 Toward negative Poisson ratio polymers through molecular design. *Macromolecules* **31**, 3145–3147. (doi:10.1021/ma970787m)

He, C., Liu, P., McMullan, P. J. & Griffin, A. C. 2005 Toward molecular auxetics: main chain liquid cyrstalline polymers consisting of laterally attached para-quaterphenyls. *Phys. Status Solidi B Basic Res.* **242**, 576–584. (doi:10.1002/pssb.200460393)

Kowalik, M. & Wojciechowski, K. W. 2005 Poisson's ratio of degenerate crystalline phases of three-dimensional hard dimmers and hard cyclic trimers. *Phys. Status Solidi B* **242**, 626–631. (doi:10.1002/pssb.200460381)

Lakes, R. S. 1987 Foam structures with a negative Poisson's ratio. *Science* **235**, 1038–1040. (doi:10.1126/science.235.4792.1038)

Lakes, R. S. & Elms, K. E. 1993 Indentability of conventional and negative Poisson's ratio foams. *J. Compos. Mater.* **27**, 1193–1202. (doi:10.1177/002199839302701203)

Lakes, R. S. & Wojciechowski, K. W. 2008 Negative compressibility, negative Poisson's ratio and stability. *Phys. Status Solidi B* **245**, 545–551. (doi:10.1002/pssb.200777708)

Lemprière, B. M. 1968 Poisson's ratio in orthotropic materials. *AIAA J.* **6**, 2226–2227. (doi:10.2514/3.4974)

Masters, I. G. & Evans, K. E. 1996 Models for the elastic deformation of honeycombs. *Compos. Struct.* **35**, 403–422. (doi:10.1016/S0263-8223(96)00054-2)

McDonald, S. A., Ravirala, N., Withers, P. J. & Alderson, A. 2009 *In situ* three-dimensional X-ray microtomography of an auxetic foam under tension. *Scr. Mater.* **60**, 232–235. (doi:10.1016j/j.scriptamat.2008.10.013)

Moore, B., Jaglinski, T., Stone, D. S. & Lakes, R. S. 2006 Negative incremental bulk modulus in foams. *Philos. Mag. Lett.* **86**, 651–659. (doi:10.1080/09500830600957340)

Norris, A. N. 2006 Poisson's ratio in cubic materials. *Proc. R. Soc. A* **462**, 3385–3405. (doi:10.1098/rspa.2006.1726)

Prall, D. & Lakes, R. S. 1997 Properties of a chiral honeycomb with a Poisson's ratio of—1. *Int. J. Mech. Sci.* **39**, 305–314. (doi:10.1016/S0020-7403(96)00025-2)

Ravirala, N., Alderson, A., Alderson, K. L. & Davies, P. J. 2005 Auxetic polypropylene films. *Polym. Eng. Sci.* **45**, 517–528. (doi:10.1002/pen.20307)

Rothenburg, L., Berlin, A. A. & Bathurst, R. J. 1991 Microstructure of isotropic materials with negative Poisson's ratio. *Nature* **354**, 470–472. (doi:10.1038/354470a0)

Sanchez-Valle, C., Sinogeikin, S. V., Lethbridge, Z. A. D., Walton, R. I., Smith, C. W., Evans, K. E. & Bass, J. D. 2005 Brillouin scattering study on the single-crystal elastic properties of natrolite and analcime zeolites. *J. Appl. Phys.* **98**, 053508. (doi:10.1063/1.2014932)

Scarpa, F. 2010 Preface to Special Issue on CHISMACOMB (CHIral SMArt honeyCOMB). *Compos. Sci. Technol.* **70**, 1033. (doi:10.1016/j.compscitech.2010.02.027)

Scarpa, F., Dallocchio, F. & Ruzzene, M. 2003 Identification of acoustic properties of auxetic foams. *Smart Struct. Mater. Conf.* 468–474. (doi:10.1117/12.487559)

Scarpa, F., Ciffo, L. G. & Yates, Y. R. 2004 Dynamic properties of high structural integrity auxetic open-cell foam. *Smart Mater. Struct.* **13**, 49–56. (doi:10.1088/0964-1726/13/1/006)

Scarpa, F., Pastorino, P., Garelli, A., Patsias, S. & Ruzzene, M. 2005 Auxetic compliant flexible PU foams: static and dynamic properties. *Phys. Status Solidi B* **242**, 681–694. (doi:10.1002/pssb.200460386)

Sigmund, O. 1995 Tailoring materials with prescribed elastic properties. *Mech. Mater.* **20**, 351–368. (doi:10.1016/0167-6636(94)00069-7)

Tretiakov, K. V. & Wojciechowski, K. W. 2007 Poisson's ratio of simple planar 'isotropic' solids in two dimensions. *Phys. Status Solidi B* **244**, 1038–1046. (doi:10.1002/pssb.200572721)

Webber, R. S., Alderson, K. L. & Evans, K. E. 2008 A novel fabrication route for auxetic polyethylene, part 2: mechanical properties. *Polym. Eng. Sci.* **48**, 1351–1358. (doi:10.1002/pen.21110)

Williams, J. L. & Lewis, J. L. 1982 Properties and an anisotropic model of cancellous bone from the proximal tibia epiphysis. *J. Biomech. Eng.* **104**, 50–56. (doi:10.1115/1.3138303)

Wojciechowski, K. W. 1989 Two-dimensional isotropic system with a negative Poisson's ratio. *Phys. Lett. A* **137**, 60–64. (doi:10.1016/0375-9601(89)90971-7)

Wojciechowski, K. W. & Branka, A. C. 1994 Auxetics: materials and models with negative Poisson's ratios. *Mol. Phys. Rep.* **6**, 71–85.

Yeganeh-Haeri, A., Weidner, D. J. & Parise, J. B. 1992 Elasticity of α-cristobalite: a silicon dioxide with a negative Poisson's ratio. *Science* **257**, 650–652. (doi:10.1126/science.257.5070.650)